^1H_2O $T_{1\rho}$ contrast generated by adiabatic HS*n* pulses in human brain 4 T images. Dipolar cross-correlation in tissue.

S. Michaeli[1], D. J. Sorce[1], C. S. Springer[2], K. Ugurbil[1], M. Garwood[1]

[1]Department of Radiology, CMRR, University of Minnesota, Minneapolis, MN, United States, [2]Oregon Health & Science University, Advanced Imaging Research Center, Portland, Oregon, United States

Introduction Recently we have demonstrated that transverse relaxation in the rotating frame ($T_{2\rho}$) is the dominant relaxation pathway during an adiabatic Carr-Purcell (CP) spin-echo pulse sequence with no delays between AFP pulses [1]. Exchange-induced $T_{2\rho}(T_{2\rho ex})$ and the contribution of dipolar interactions ($T_{2\rho,dd}$) were found to depend on the adiabatic pulse modulation functions used. This was utilized to modulate ^1H_2O $T_{2\rho}$ contrast in images of the human occipital lobe at 4T. It was shown that dynamic averaging (DA), e.g., equilibrium water exchange and diffusion in locally different magnetic susceptibilities, is the major mechanism accounting for the $T_{2\rho}$ dependence on the AFP pulse modulation functions of the hyperbolic secant HS*n* (n = 1,4) family. Here we investigate adiabatic $T_{1\rho}$ contrast, which is generated by placing a train of HS1 or HS4 pulses prior to the AHP excitation pulse with no interpulse intervals. Our study shows that adiabatic $T_{1\rho}$ contrast originates from dipolar cross-correlations (e.g., interference between dipolar relaxation pathways), and the DA mechanism has just a minor contribution to the ^1H_2O $R_{1\rho}$ relaxation rate constants in human brain tissue. Adiabatic $T_{1\rho}$ contrast provides a possibility to directly assess dipolar type of interactions (i.e., cross-correlations) in living tissue.

Methods Imaging studies were conducted with a 4T whole body MRI/MRS system. A ^1H quadrature surface coil consisting of two geometrically decoupled turns (each 7 cm in diameter) was used for the measurements. HS1 and HS4 AFP pulses were inserted prior to the adiabatic half passage pulse of the sequence. $T_{1\rho}$ images were acquired incrementing the number of AFP pulses (pulse length 3 ms, ω_1^{max}=2.5 kHz). Spiral readout (0.7 x 0.7 mm^2 in-plane resolution, FOV = 18 cm, 256-matrix and 8 segments, at = 35 ms, thickness 3 mm) was used for the acquisition. $T_{1\rho}$-maps were generated to analyze the experimental data. Slice-selection was performed with two HS1 pulses applied in the presence of slice selection gradients, after non-selective excitation with an adiabatic half-passage (AHP) pulse. TR = 7 s was used.

Results and Discussion

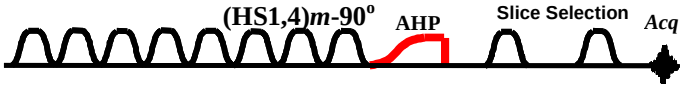

Figure 1. Schematic representation of the adiabatic pulse sequence used for the $T_{1\rho}$ measurements.

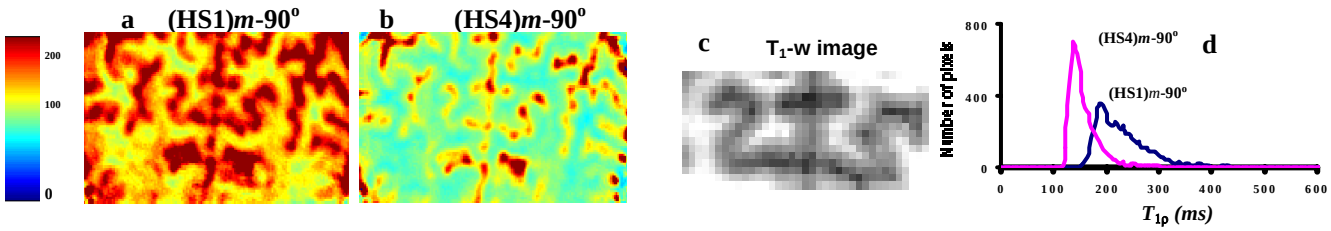

Figure 2. $T_{1\rho}$ maps (a,b) generated from single-subject measurements, detected with the (a) (HS1)*m*-90° and (b) (HS4)*m*-90° pulse sequences (Figure 1); (c) identical ROI of the T_1 -weighted image; (d) $T_{1\rho}$ relaxograms of a human brain image slice in the occipital lobe, generated from the $T_{1\rho}$ maps.

^1H_2O NMR relaxation in tissue arises from complicated molecular mechanisms that include equilibrium water exchange and magnetic interactions between the protons of different molecular constituents in several tissue compartments. To simulate this, we use a simple, two-site model that represents two water populations. These two reservoirs are coupled by the two-site exchange (2SX) mechanism. In our interpretation three major issues are considered: 1) the orientational order of ^1H dipolar interactions and its contribution to the relaxation dispersion; 2) the effect of cross-correlations between water protons and macromolecular protons; 3) 2SX between two water populations.

In Figure 2 a,b, ^1H_2O $T_{1\rho}$ maps generated from measurements using the (a) (HS1)*m*-90° and (b) (HS4) *m*-90° pulse sequences are presented. It can be seen that $T_{1\rho}$ relaxation is significantly affected by the adiabatic pulse modulation functions used. In this study, the ratio $T_{1\rho}$ ((HS1)*m*-90°)/ $T_{1\rho}$ ((HS4)*m*-90°) ≈ 1.51 (±0.15) was obtained (5 individuals). The anisochronous $T_{1\rho,ex}$ contribution (e.g., exchange between spins with different resonance frequencies; $\delta\omega \neq 0$) during the HS1 and HS4 pulses was estimated using the referenced relaxation equations and the parameters obtained from 4T human brain ^1H_2O relaxation data [2]. This analysis suggested that the relaxation rate constants $R_{1\rho,ex}$ (HS1,HS4) due to CE in human brain are small. This in turn implies that dipolar relaxations dominate under these experimental conditions (ω_1^{max} = 2.5 kHz, pulse length T_p = 3 ms). In this work, the formalism for the three-spin system dipolar cross-correlations $R_{1\rho,cc}$ was implemented for the HS1 (a) and HS4 (b) pulses, respectively [3]. The dependences of $R_{1\rho,cc}$ on the rotational correlation times τ_c during the HS1 and HS4 pulse are presented on Figure 3. In this work, the formalisms of dipolar cross-correlations and isochronous 2SX (e.g. exchange between spins at sites A and B with identical resonance frequencies and different relaxation times T_{2A} and T_{2B} in the absence of exchange) were used to describe the adiabatic $T_{1\rho}$ contrast.

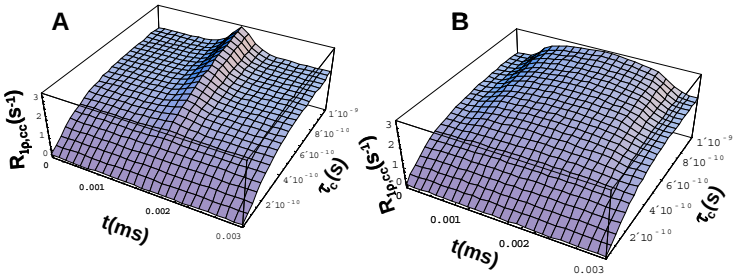

Figure 3. Calculated ^1H_2O longitudinal relaxation rate constant ($R_{1\rho cc}$) during the A) HS1 and B) HS4 pulses as a function of the rotational correlation time (τ_c). The pulse parameters used for calculation were: pulse length T_p = 0.003 s, R = 20, ω_1^{max} = 2.5 kHz.

Conclusion We have demonstrated that modified adiabatic $T_{1\rho}$ contrast can be generated in human brain ^1H_2O images based on differences in the adiabatic pulse modulation functions used. This relaxation contrast provides a direct assessment of dipolar cross-correlations in tissue. This information is *unique* for investigation and characterization of the ^1H_2O relaxation mechanisms *in vivo*. Adiabatic $T_{1\rho}$ contrast holds great potential for investigation, characterization and diagnosis of neurodegenerative disorders, cancer and stroke.

References [1] Michaeli S, Sorce DJ, Idiyatullin D, Ugurbil K, Garwood M. *J Magn Reson* **169**:293-299 (2004); [2] Michaeli S, Grohn H, Grohn O, Sorce DJ, Kauppinen R, Springer C, Ugurbil K, Garwood M. accepted for *Magn Reson Med* (2004); [3] Burghardt I, Konrat R, Bodenhausen G *Mol Phys*, 75, 467-486 (**1992**).

Acknowledgment This work was supported by NIH grants CA92004, RR08079, NS40801, and EB00422, the Keck Foundation, and the Mind Institute.